

Sugar Ring Distortion in the Glycosyl-Enzyme Intermediate of a Family G/11 Xylanase^{†,‡}

Gary Sidhu,^{§,||} Stephen G. Withers,^{||,⊥} Nham T. Nguyen,^{||} Lawrence P. McIntosh,^{||,⊥} Lothar Ziser,^{⊥,∇} and Gary D. Brayer^{*,||}

Department of Biochemistry and Molecular Biology, University of British Columbia, Vancouver V6T 1Z3, Canada, and Department of Chemistry, University of British Columbia, Vancouver V6T 1Z1, Canada

Received December 15, 1998

ABSTRACT: The 1.8 Å resolution structure of the glycosyl-enzyme intermediate formed on the retaining β -1,4-xylanase from *Bacillus circulans* has been determined using X-ray crystallographic techniques. The 2-fluoro-xylose residue bound in the -1 subsite adopts a ^{2.5}B (boat) conformation, allowing atoms C5, O5, C1, and C2 of the sugar to achieve coplanarity as required at the oxocarbenium ion-like transition states of the double-displacement catalytic mechanism. Comparison of this structure to that of a mutant of this same enzyme noncovalently complexed with xylotetraose [Wakarchuk et al. (1994) *Protein Sci.* 3, 467–475] reveals a number of differences beyond the distortion of the sugar moiety. Most notably, a bifurcated hydrogen bond interaction is formed in the glycosyl-enzyme intermediate involving H ^{η} of Tyr69, the endocyclic oxygen (O5) of the xylose residue in the -1 subsite, and O ^{ϵ 2} of the catalytic nucleophile, Glu78. To gain additional understanding of the role of Tyr69 at the active site of this enzyme, we also determined the 1.5 Å resolution structure of the catalytically inactive Tyr69Phe mutant. Interestingly, no significant structural perturbation due to the loss of the phenolic group is observed. These results suggest that the interactions involving the phenolic group of Tyr69, O5 of the proximal saccharide, and Glu78 O ^{ϵ 2} are important for the catalytic mechanism of this enzyme, and it is proposed that, through charge redistribution, these interactions serve to stabilize the oxocarbenium-like ion of the transition state. Studies of the covalent glycosyl-enzyme intermediate of this xylanase also provide insight into specificity, as contacts with C5 of the xylose moiety exclude sugars with hydroxymethyl substituents, and the mechanism of catalysis, including aspects of stereoelectronic theory as applied to glycoside hydrolysis.

The endo-1,4- β -xylanases of family G/11 are enzymes involved in the hydrolysis of nature's most abundant hemicellulose, xylan (2). These low molecular weight xylanases perform this function with net retention of anomeric configuration and thus employ the double-displacement catalytic mechanism of retaining β -glycosidases (3). In this mechanism, hydrolysis proceeds through a glycosyl-enzyme intermediate that is formed and hydrolyzed via transition states with substantial oxocarbenium ion character (4, 5). Interest in the mechanism of β -1,4-xylanases has been piqued with the realization that these enzymes are excellent targets for protein engineering experiments. Xylanolytic activity is

useful in biotechnological applications such as the bleaching of hardwood kraft pulp for paper manufacture and the processing of feed for livestock (6, 7).

A substantial volume of both structural and functional information is now available on the family G/11 xylanases (8). The three-dimensional fold of five of these enzymes has been determined, and the two acidic residues implicated in the double-displacement mechanism have been identified through a combination of sequence analysis, mutational studies, inhibition experiments, and structure determination (9–15). In the case of *Bacillus circulans* xylanase (BCX¹), NMR experiments involving both the native enzyme and a glycosyl-enzyme intermediate have even allowed for the determination of pK_a changes that accompany the enzymatic reaction (16). Nevertheless, there is a lack of detailed information regarding the reaction pathway that prevents a thorough understanding of the mechanism of xylanase

[†] This work was funded by the Government of Canada's Network of Centres of Excellence program supported by the Medical Research Council of Canada (MRC) and the Natural Sciences and Engineering Research Council (NSERC) through the Protein Engineering Network of Centres of Excellence (PENEC).

[‡] Coordinates for the structures described in this work have been deposited in the Brookhaven Protein Data Bank (1) (Accession numbers 1bvj and 2bvj).

* To whom correspondence should be addressed. Tel: 604-822-5216. Fax: 604-822-5227. Email: brayer@laue.biochem.ubc.ca.

[§] Gary Sidhu is a recipient of an NSERC Postgraduate Scholarship.

^{||} Department of Biochemistry and Molecular Biology.

[⊥] Department of Chemistry.

[∇] Present address: GlycoDesign Inc., 480 University Avenue, Toronto, Ontario, Canada M5G 1V2.

¹ Abbreviations: BCX, *Bacillus circulans* xylanase; DNPFXb, 2',4'-dinitrophenyl 2-deoxy-2-fluoro- β -xylobioside; 2FXb, 2-deoxy-2-fluoro-xylobiose; BCX-2FXb, 2-deoxy-2-fluoro xylobiosyl enzyme intermediate of *Bacillus circulans* xylanase; BCX-Xb, noncovalent complex of *Bacillus circulans* xylanase and xylotetraose; Y69F BCX, *Bacillus circulans* xylanase with Tyr69 substituted by Phe; R112K BCX, *Bacillus circulans* xylanase with Arg112 substituted by Lys; R112N BCX, *Bacillus circulans* xylanase with Arg112 substituted by Asn.

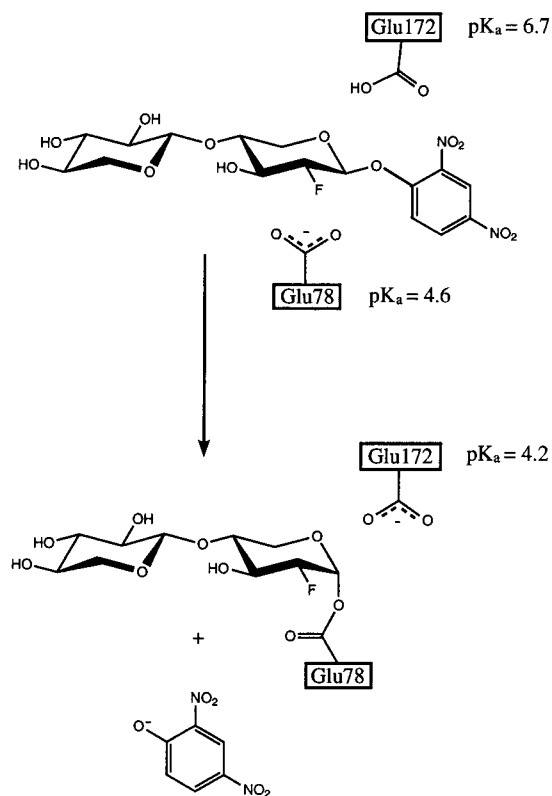


FIGURE 1: Schematic representation of the formation of the glycosyl-enzyme intermediate species on BCX. The fluorine atom at position 2 of the proximal saccharide slows both the formation and the hydrolysis of the intermediate. The 2,4-dinitrophenyl leaving group, however, facilitates the first nucleophilic attack by Glu78, allowing the intermediate to form. The pK_a 's of Glu78 and Glu172 have been determined by NMR methods (16).

catlysis. The structure of a catalytically inactive BCX mutant incubated with xyloetraose has been characterized, but only a xylobiose moiety could be observed at the active site (12). Structures of epoxyalkyl xylosides covalently attached to the active site residues of xylanase II from *Trichoderma reesei* are also available, but these include only one xylose residue (17).

Detailed structural information on a glycosyl-enzyme intermediate would provide valuable insight into the catalytic mechanism of BCX. Such an intermediate can be trapped using the mechanism-based inhibitor (or "slow substrate") 2',4'-dinitrophenyl 2-deoxy-2-fluoro- β -xylobioside (DNPFb), as has been done in kinetic and spectroscopic studies (Figure 1) (15, 16). The electronegative fluorine atom at the 2-position of the xylose moiety slows both the formation and the hydrolysis of the intermediate by inductively destabilizing the oxocarbenium ion-like transition states and by eliminating important hydrogen-bonding interactions at this position (18, 19). The 2,4-dinitrophenyl leaving group, however, facilitates the first nucleophilic attack by Glu78 and thus allows the intermediate to form with a second-order rate constant, k_f/K_i , of $0.34 \text{ min}^{-1} \text{ mM}^{-1}$ at 40°C and pH 6.0 (15). The intermediate then slowly hydrolyzes with $t_{1/2} = 350 \text{ min}$ under these conditions. Recently, similar inhibitors have been used in X-ray crystallographic studies of other glycosyl-enzyme complexes, including those formed on the catalytic domain of the β -1,4-glycanase Cex from *Cellulomonas fimi*, the S-glycosidase myrosinase from *Sinapis alba*, and the cellulase Cel5A from

Bacillus agaradherens (20–23). The results of these experiments confirm a double-displacement mechanism by showing unambiguously the covalent linkage between the catalytic nucleophile and the sugar moiety. All three enzymes belong to the GH-A clan and, as such, possess the same $(\beta/\alpha)_8$ TIM barrel fold and conserved catalytic machinery (2). Information regarding glycosyl-enzyme intermediates of enzymes outside of this clan has not been reported and may well provide new insight into glycosidase catalytic mechanisms.

Our efforts have focused on determining the structure of the glycosyl-enzyme intermediate formed on a family G/11 xylanase in order to gain a better understanding of the substrate specificity and catalytic mechanism of this enzyme. We have used the xylanase from *Bacillus circulans* and the DNPFb inhibitor to generate the glycosyl-enzyme intermediate (BCX–2FXb) and have elucidated the structure of this species using X-ray crystallographic techniques. Furthermore, to probe the function of a critical residue at the active site, we have also determined the structure of BCX with Tyr69 replaced by Phe (Y69F BCX). The results of these studies provide a unique glimpse into structural aspects of the catalytic mechanism of enzymes from this family and insight into the role of substrate distortion in enzyme catalysis.

EXPERIMENTAL PROCEDURES

Materials. The mechanism-based inhibitor was synthesized as described previously (24). Enzyme mutagenesis, expression, and purification were performed using reported protocols (12).

Crystallization and Soaking. Crystals of both wild type and Y69F BCX were grown at room temperature (21°C) using the hanging drop vapor diffusion method. The reservoir solution contained 17% $(\text{NH}_4)_2\text{SO}_4$, 10 mM NaCl, and 40 mM Tris HCl at pH 7.5. The hanging droplets consisted of $5 \mu\text{L}$ of protein solution (15 mg mL^{-1}) mixed with $5 \mu\text{L}$ of reservoir solution. Diffraction quality crystals appeared after 1 month. Wild-type BCX crystals were soaked in a $75 \mu\text{L}$ aliquot of well solution which was combined with $25 \mu\text{L}$ of 1.5 mM DNPFb, 100% $(\text{NH}_4)_2\text{SO}_4$, 10 mM NaCl, and 40 mM Tris HCl at pH 7.5 for 28 h just prior to data collection.

Structure Determination. Diffraction data were collected on a Rigaku R-AXIS IIC imaging plate area detector system using Cu $K\alpha$ radiation supplied by a Rigaku RU300 rotating anode generator operating at 50 kV and 100 mA. Each diffraction data frame was exposed for 20 min during which time the crystal was oscillated through 1.2° . Intensity data were then integrated, scaled, and reduced to structure factor amplitudes with the HKL suite of programs (25). Data collection statistics are provided in Table 1.

Since crystals of both BCX–2FXb and Y69F BCX retained isomorphous unit cells with that of wild-type BCX, the wild-type BCX structural model (with Tyr69 truncated to alanine for Y69F BCX) was used to phase diffraction data (11). These starting models were subjected to rigid body, simulated annealing, positional, and individual isotropic thermal factor refinement using X-PLOR (26) and the CCP4 Suite (27) until convergence was realized. At this point, $F_o - F_c$ difference electron density maps were calculated and the 2FXb disaccharide and Phe69 residue were built with the program O (28) into the density observed for BCX–

Table 1: Data Collection Parameters for BCX-2FXb and Y69F BCX

parameters	BCX-2FXb	Y69F BCX
space group	$P2_12_12_1$	$P2_12_12_1$
cell dimensions (Å)		
a	43.87	44.00
b	52.79	52.75
c	78.09	78.49
no. of measurements	137937	128221
no. of unique reflections	17727	30126
mean I/σ^a	13.6 (4.9)	16.2 (3.6)
merging R -factor (%) ^{a,b}	7.3 (30.3)	6.4 (19.9)
resolution range (Å)	∞ -1.8	∞ -1.5

^a Values in parentheses are for the last resolution shell (1.86-1.80 Å for BCX-2FXb and 1.55-1.50 Å for Y69F BCX). ^b $R_{\text{merge}} = \sum_{i=0}^n |I_i - \bar{I}_{hkl}| / \sum_{i=0}^n I_{hkl}$.

Table 2: Refinement Statistics for BCX-2FXb and Y69F BCX

parameters	BCX-2FXb	Y69F BCX
no. of reflections	17492	27832
resolution range (Å)	10-1.8	10-1.5
completeness within range (%)	99.0	92.7
no. of protein atoms	1427	1426
no. of ligand atoms	18	
no. of solvent atoms	117	148
average thermal factors (Å ²)		
protein atoms	14.4	12.5
ligand atoms	17.6	
solvent atoms	34.7	34.7
final refinement R -factor (%) ^a	18.9	18.8
stereochemistry	rms deviations	
bonds (Å)	0.007	0.007
angles (deg)	1.128	1.155

^a $R\text{-factor} = \sum_{hkl} |F_o - F_c| / \sum_{hkl} |F_o|$.

2FXb and Y69F BCX, respectively. The models were then refined further with X-PLOR using the standard protein and carbohydrate topology and parameter libraries. Because the electron density in BCX-2FXb clearly indicated that the conformation of the proximal saccharide was distorted, the dihedral angle restraints on this residue were removed. The length of the new glycosidic bond formed to Glu78 was restrained to a value of 1.43 Å using a weight similar to that applied to other sugar bond lengths in the ligand (20). Atoms of the bound disaccharide were refined at full occupancy. The models were examined periodically during the refinement with $F_o - F_c$, $2F_o - F_c$, and fragment-deleted difference electron density maps. Manual adjustments were made as necessary, and solvent molecules were identified. The validity of solvent molecules was assessed on the basis of both hydrogen-bonding potential to appropriate protein atoms and refinement of a thermal factor of less than 75 Å². The final R -factors for BCX-2FXb and Y69F BCX are 18.9% and 18.8%, while the coordinate errors, as estimated from a Luzzati plot, are 0.18 and 0.17 Å, respectively (Table 2) (29).

RESULTS AND DISCUSSION

Conformation of the Covalently Bonded Disaccharide and the Neighboring Active Site Residues. The structure of the BCX-2FXb glycosyl-enzyme intermediate was determined to a resolution of 1.8 Å (Table 1, Figure 2). The final refined model exhibits excellent stereochemistry (Table 2). The

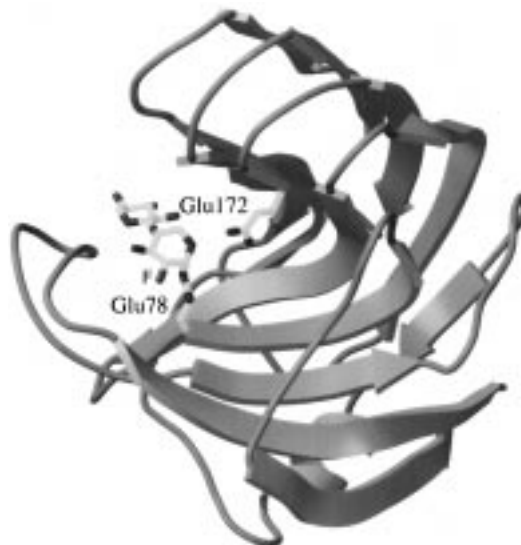


FIGURE 2: The three-dimensional structure of the BCX-2FXb glycosyl-enzyme intermediate. Along with the bound disaccharide, the side chains of the two glutamate residues implicated in the double-displacement mechanism are shown. Where individual bonds are depicted, heteroatoms are shown in black and carbon atoms are shown in light gray. The fluorine atom is labeled. Relative to native BCX, atoms in the polypeptide chain loop (residues 111-125) to the left of the bound inhibitor have shifted away from the active site cleft to accommodate the disaccharide moiety. Figures 2, 4, 5a, and 7 were generated with Bobscrip and Raster3D (47, 48).

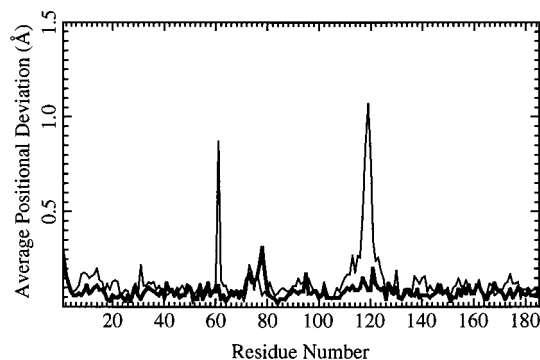


FIGURE 3: The average deviations of main chain atoms in the polypeptide chains of BCX-2FXb (thin line) and Y69F BCX (thick line) from those of wild-type BCX (11). The BCX-2FXb and wild-type structures were superimposed by least-squares fitting the positions of main chain atoms in residues 1-110 and 126-185, while the Y69F BCX and wild-type structures were superimposed by fitting all main chain atoms.

bound disaccharide atoms refine well with an average thermal factor of 17.6 Å², comparable to the value of 14.4 Å² for all protein atoms. Differences observed in the BCX-2FXb structure relative to the free enzyme as determined by Campbell et al. (11) are primarily restricted to the flexible loop region, composed of residues 111-125, at the entrance of the active site (Figure 3). Residues in this loop shift up to 1 Å, leading to a widening of the active site cleft. A small change in the position of Gly61 is also observed. The electron density for this region suggests the presence of two conformations, with that included in the final model being best defined for BCX-2FXb.

The final refined enzyme-intermediate structure shows the 2-deoxy-2-fluoro-xylobiose (2FXb) ligand covalently bonded to the nucleophile, Glu78, via an α -anomeric linkage with

the C1 atom of the proximal saccharide syn to the newly formed ester group (Figure 4). The proximal saccharide occupies the -1 subsite (30) of BCX, and the new bond between the C1 atom and the O^{e2} atom of Glu78 is 1.45 Å in length. The observation of the covalent glycosyl-enzyme intermediate confirms the double-displacement mechanism shown in Figure 1.

The xylose residue covalently bonded to Glu78 is heavily distorted from the conventional ⁴C₁ (chair) conformation and adopts instead a ^{2.5}B (boat) conformation (Figure 4) (31). The ^{2.5}B conformation of the proximal saccharide allows its C5, O5, C1, and C2 atoms to achieve a nearly planar geometry (0.05 Å rms deviation from planarity versus 0.22 Å rms deviation for the same atoms in the distal saccharide). These results mark the first crystallographic observation of such significant distortion in a glycosyl-enzyme complex. The distal xylose residue in the -2 subsite maintains a ⁴C₁ conformation and makes van der Waals contacts with the main chain atoms of Ser117 and a stacking interaction with the side chain atoms of Trp9 in a fashion similar to that observed in the noncovalent BCX-xylobiose (BCX-Xb) complex structure (Figure 5) (12). Stacking interactions of this type have been observed in other carbohydrate-protein complexes (32).

The planarity observed for the C5, O5, C1, and C2 atoms of the proximal saccharide in the ^{2.5}B conformation is of particular interest. As noted earlier, both steps of the reaction catalyzed by BCX proceed through transition states with substantial oxocarbenium ion-like character in which a partial double bond develops between O5 and C1 (33). This requires C5, O5, C1, and C2 to approach coplanarity at the transition state. Since such planarity is realized at the glycosyl-enzyme intermediate, the formation and hydrolysis of this species should be considerably facilitated.

Although the rearrangements involved in generating a ^{2.5}B conformation from a ⁴C₁ may appear considerable, they can occur with little perturbation of the relative positions of most atoms of the proximal saccharide. If the rearrangement proceeds via a ⁴C₁ → ²H₃ → ²S₀ → ^{2.5}B itinerary (34), the relative movement is confined mostly to atoms C5 and O5. In this case, the dihedral angle defined by atoms C1, C2, C3, and C4 is not required to undergo much change (this angle is observed to be 48° in the proximal saccharide and 57° in the distal saccharide). Note that the C5 and O5 atoms of xylose are not encumbered by the functional groups found on atoms C1, C2, C3, and C4 and thus are able to experience the movement prescribed by the aforementioned rotational itinerary without a large energetic cost.

The acid/base catalyst, Glu172, occupies a similar position and conformation in the BCX-2FXb complex to that found in the wild-type BCX structure (11). The O^{e2} atom of Glu172, which both donates and abstracts protons during catalysis, makes a 3.10 Å hydrogen bond to a water molecule situated 3.92 Å away from the C1 atom of the proximal saccharide (Figure 6). This water molecule is also hydrogen bonded to the phenolic oxygen atom of Tyr80 ($d = 2.74$ Å), as well as to a second solvent molecule ($d = 3.17$ Å), and is a likely candidate for the nucleophile in the deglycosylation step of the reaction. According to the proposed mechanism and recent pK_a measurements, the O^{e2} atom of Glu172 is deprotonated under experimental conditions (pK_a = 4.2) and thus must accept a hydrogen bond from the nearby water

molecule (16, 35). Tyr80, which appears to be donating a hydrogen bond ($d = 2.83$ Å) to the deprotonated O^{e1} atom of Glu172, must then also accept a hydrogen bond from the water molecule. In this position, one of the lone pairs of the tetrahedral oxygen atom of this water molecule is directed toward the second solvent molecule while the other lone pair points in the general direction of the proximal saccharide. This placement is ideal for an attack on the C1 atom of the proximal saccharide residue during the deglycosylation reaction (Figure 6).

Comparison of BCX-2FXb, BCX-Xb, and Y69F BCX. It is instructive to compare the enzyme-ligand interactions observed in the BCX-2FXb glycosyl-enzyme intermediate with those of the BCX-Xb noncovalent complex for which the xylobiose moiety is also bound in the -1 and -2 subsites. Note that the crystals for the noncovalent complex were soaked with xylotetraose, yet only two xylose residues were observed (12). Both xylose residues in the BCX-Xb complex maintain ⁴C₁ conformations, thus placing the nucleophilic oxygen atom of Glu78 3.35 Å from the anomeric carbon of the proximal saccharide (Figure 4c). The requirement to shorten this distance to the length of a glycosidic bond must be an important driving force for the ⁴C₁ → ^{2.5}B conformational rearrangement of the proximal xylose residue.

When comparing the BCX-2FXb and BCX-Xb structures, interactions with Tyr69 are of particular interest (Table 3). In the noncovalent complex, this residue donates a strong hydrogen bond ($d = 2.60$ Å) to the nucleophilic oxygen atom (O^{e2}) of Glu78 and accepts a hydrogen bond from the 2-position OH of the distal xylose moiety. In contrast, in the covalent intermediate, the hydrogen bond donated to the O^{e2} atom of Glu78 is weaker ($d = 2.99$ Å), consistent with the ether character of its partner. Furthermore, a new interaction for the phenolic oxygen of Tyr69 is formed in BCX-2FXb with the endocyclic oxygen (O5) of the proximal xylose moiety (Figures 5 and 6). The nature of this interaction is intriguing since the hydroxyl group of Tyr69 is very important for catalysis, as evident by the fact that the Y69F variant of BCX exhibits no detectable enzyme activity (M. D. Joshi, personal communication) (12). A similar interaction is also observed in the 2-fluoroglucosyl-enzyme complex of the Family 1 *Sinapis alba* myrosinase (22). In that case, Tyr330 moves upon formation of the complex such that its hydroxyl group points toward the sugar ring oxygen. This residue is completely conserved in Family 1, and indeed, the Phe mutant at the corresponding position in the β-glucosidase from *Agrobacterium sp.* (Tyr298) has 2000-fold lower activity than the wild-type enzyme, pointing to an important role (36).

To further understand the catalytic function of Tyr69, we determined the structure of the Y69F variant of BCX to 1.5 Å resolution (Tables 1 and 2). This substitution at position 69 has little effect on the overall three-dimensional fold of BCX (Figure 3). The rms deviation for main chain atoms is 0.09 Å and for all atoms is 0.26 Å relative to the wild-type enzyme. On the basis of earlier hypotheses that Tyr69 played a crucial role in positioning Glu78 (12), it might have been expected that the loss of the hydrogen bond from Tyr69 to Glu78 in Y69F BCX would alter the position of the nucleophile carboxylate and thereby disrupt catalysis. It is

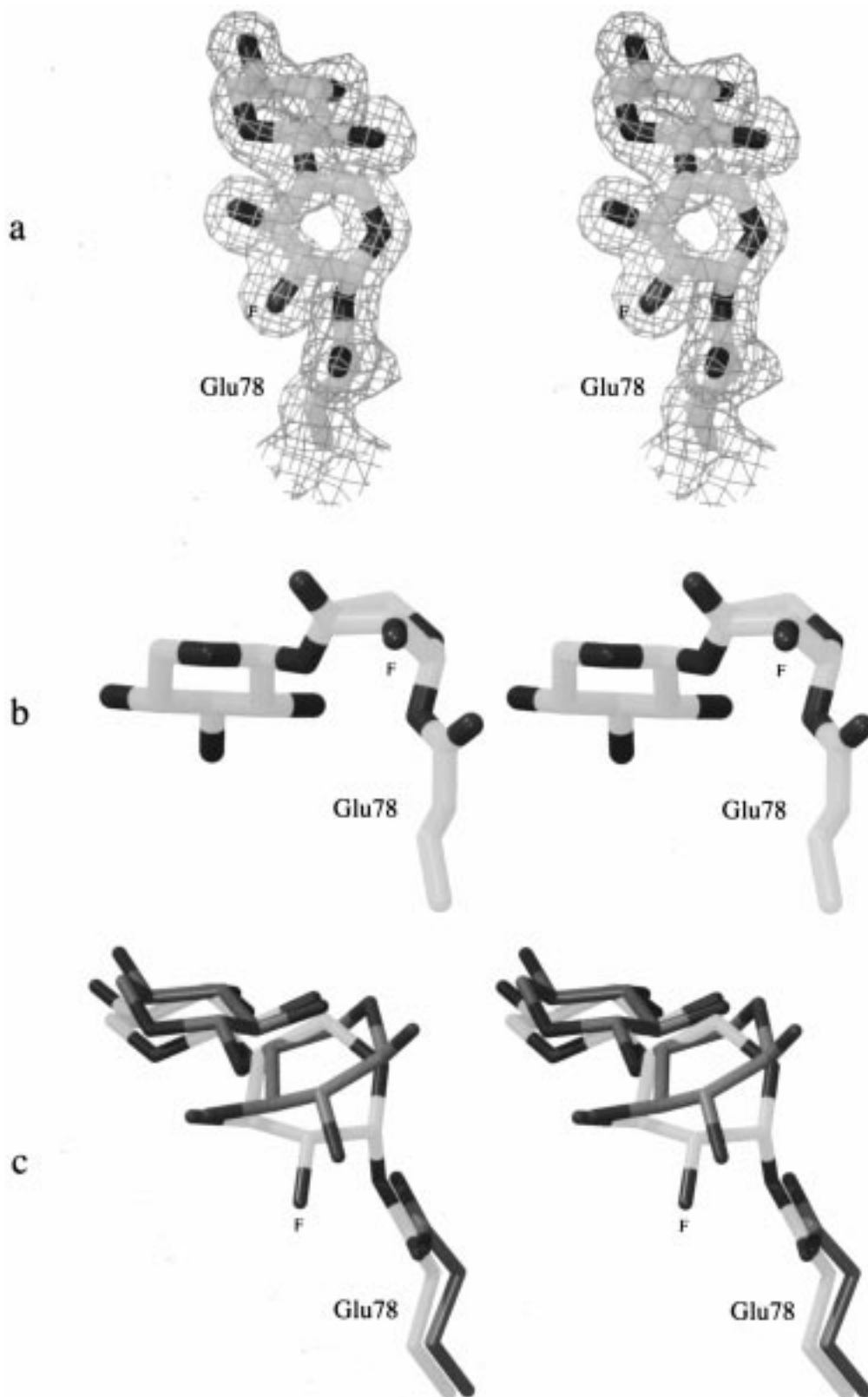


FIGURE 4: Stereo diagrams depicting the conformation of the 2FXb disaccharide of the intermediate. (a) The disaccharide ligand superimposed on an $F_o - F_c$ difference electron density map calculated before the inclusion of the ligand atoms in the refinement model and with Glu78 omitted from F_c . This map is contoured at the 2σ level. (b) An alternative orientation showing Glu78 and the proximal residue of the disaccharide which adopts a ${}^2.5B$ conformation. The distal residue maintains a 4C_1 conformation. Atom shading for (a) and (b) follows the conventions of Figure 2. (c) Stereo diagram showing the conformations of the ligands for both the BCX-2FXb and the BCX-Xb complex structures. Coordinates were superimposed by least-squares fitting the main chain atoms of residues 1-110 and 126-185. The carbon atoms belonging to the BCX-Xb noncovalent structure are depicted in dark gray, while those belonging to the BCX-2FXb glycosyl-enzyme intermediate are depicted in light gray. Heteroatoms are shown in black, and the fluorine atom is labeled.

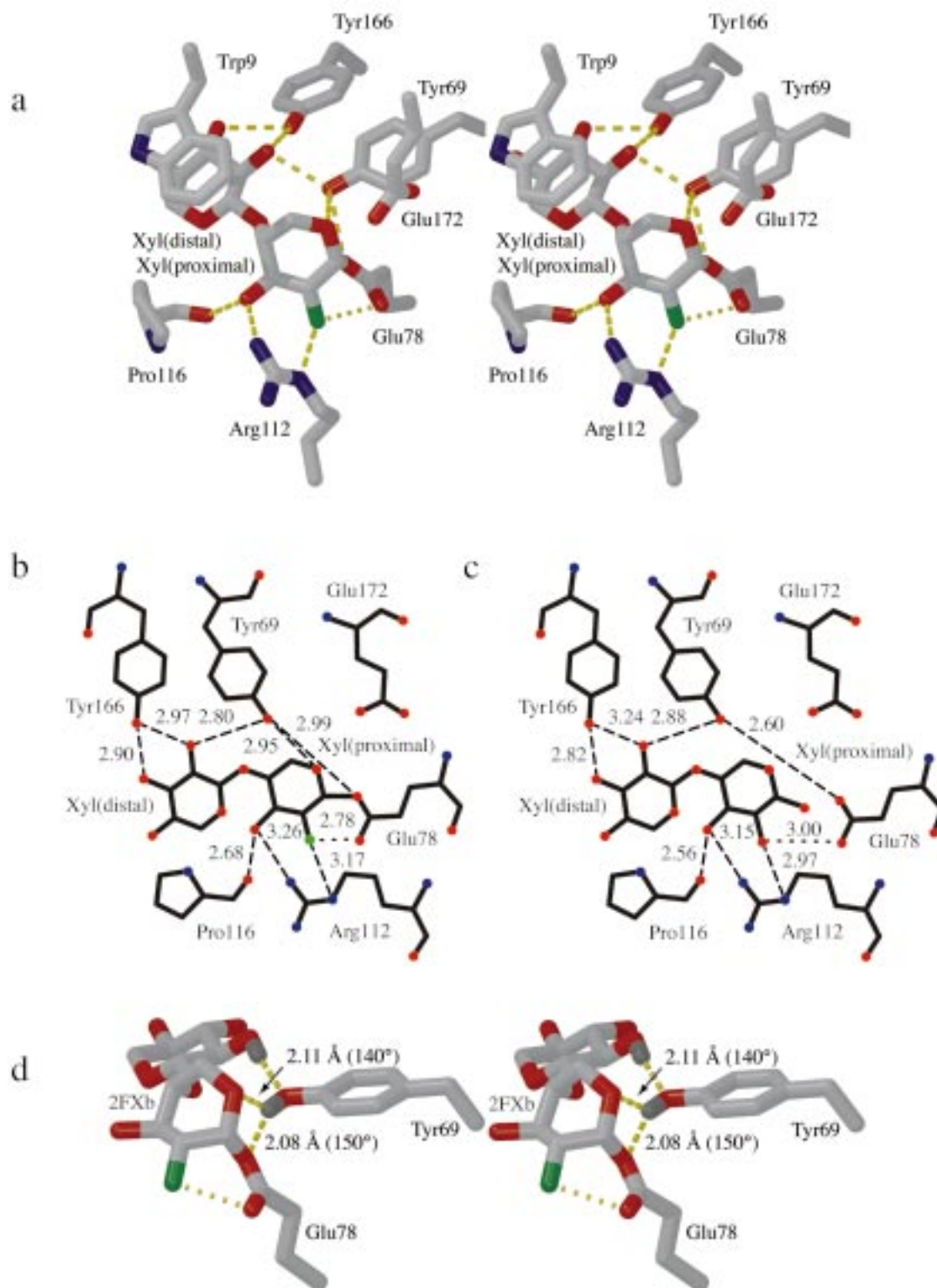


FIGURE 5: Interactions of the 2FXb disaccharide with active site residues. (a) A stereo diagram showing interactions formed in the BCX-2FXb complex. (b) A schematic detailing the interactions and distances observed in BCX-2FXb. (c) A schematic detailing the interactions and distances observed in BCX-Xb. (d) A stereo diagram showing the hydrogen-bonding interactions of the phenolic group of Tyr69 in BCX-2FXb. Distances given are for the hydrogen-bond donor-acceptor geometry, while angles are for the hydrogen bond donor-hydrogen-hydrogen bond acceptor geometry. Lines with long dashes depict hydrogen-bonding interactions, while the line with short dashes depicts the non-hydrogen-bonding interaction described in the text. Oxygen atoms are shown in red, nitrogen atoms in blue, carbon atoms in gray or black, and the fluorine atom in green. Frames (b) and (c) were generated with HBPLUS and Ligplot (49, 50). Hydrogen atoms were added at optimal positions using HBPLUS (49).

seen in the structure of Y69F BCX, however, that the positions of the side chains of both Glu78 and Trp71, which is also hydrogen bonded to Tyr69 in the wild-type enzyme,

remain essentially unperturbed (Figure 7). Therefore, the precise placement of Glu78 must be dictated by other interactions, such as those with the nearby Gln127, and the

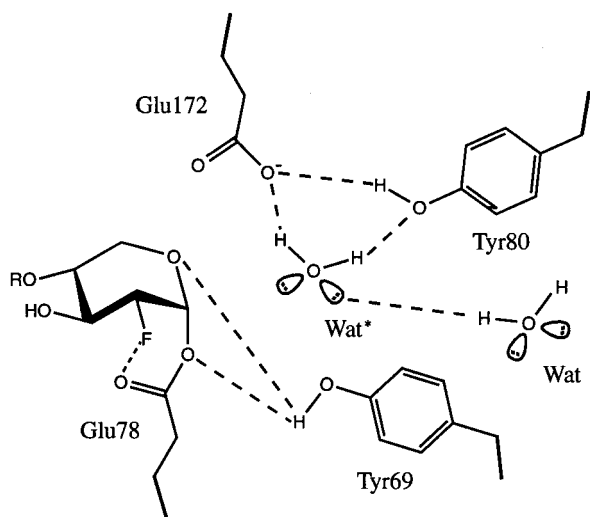


FIGURE 6: A schematic representing the observed positioning and interactions of the solvent molecule expected to act as the nucleophile (Wat^*) in the second displacement of the catalytic mechanism of BCX. Also drawn are interactions formed with the proximal saccharide residue. Lines with long dashes represent hydrogen bonds, the line with short dashes depicts the non-hydrogen bond interaction described in the text, and the R group represents the saccharide unit bound in the -2 subsite of the active site.

Table 3: Interactions at the Active Site of BCX-2FXb and BCX-Xb

interaction	distances (\AA)	
	BCX-2FXb	BCX-Xb
Tyr69 O^{η} -Glu78 $\text{O}^{\epsilon 2}$	2.99	2.60
Tyr69 O^{η} -distal Xyl O2	2.80	2.88
Tyr69 O^{η} -proximal Xyl O5	2.95	4.04
Glu78 $\text{O}^{\epsilon 1}$ -proximal Xyl O2 (F2) ^a	2.78	3.00
Arg112 N^{ϵ} -proximal Xyl O2 (F2) ^a	3.17	2.97
Arg112 $\text{N}^{\eta 2}$ -proximal Xyl O3	3.26	3.15
Pro 116 O-proximal Xyl O3	2.68	2.56
Tyr166 O^{η} -distal Xyl O2	2.97	3.24
Tyr166 O^{η} -distal Xyl O3	2.90	2.82

^a Atoms in parentheses reflect substitutions made at the 2-position of the DNPFXb ligand.

requirement of Tyr69 for catalysis must be manifest in some other fashion.

Since, in the BCX-2FXb structure, the hydroxyl group of Tyr69 donates a hydrogen bond to $\text{O}^{\epsilon 2}$ of Glu78, it cannot also donate to O5 of the proximal xylose residue unless its proton is able to alternately occupy two sites or form a bifurcated hydrogen bond (37). A detailed analysis of the hydrogen-bonding geometry about Tyr69 suggests that the latter is, in fact, quite possible. Both of the potential hydrogen bonds formed with Tyr69 H^{η} have reasonable distances and angles, as presented in Figure 5. The hydrogen bond interaction of Tyr69 with the endocyclic O5 oxygen atom of the proximal saccharide may be required to assist the conformational rearrangement and stabilize the ${}^{2,5}B$ boat conformation in the reaction intermediate. The involvement of Tyr69 in such a bifurcated hydrogen bond may also explain its necessity for catalysis. Interestingly, a study of the hydrogen-bonding geometry of Tyr330 in the glycosyl-enzyme intermediate of *Sinapis alba* myrosinase shows similar interactions of the phenolic hydroxyl group with the $\text{O}^{\epsilon 2}$ atom of the catalytic nucleophilic, Glu409, and the

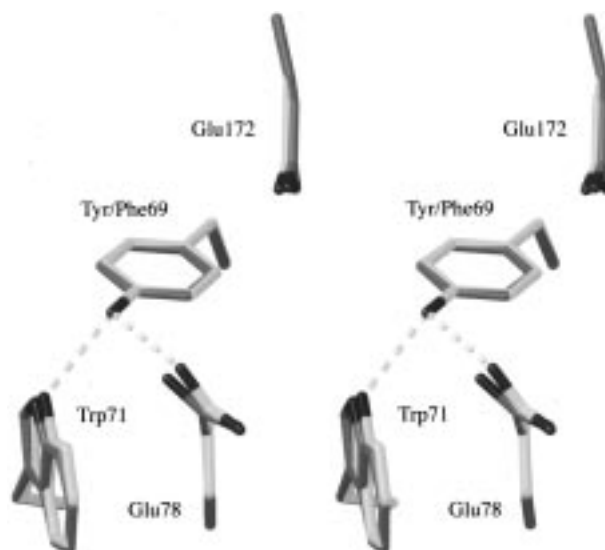


FIGURE 7: A stereo diagram comparing the conformations of active site residues of both wild type and Y69F BCX. Coordinates were superimposed by least-squares fitting all main chain atoms. Carbon atoms for the wild-type enzyme are shown in light gray, and carbon atoms of Y69F BCX are shown in dark gray. Heteroatoms are shown in black.

endocyclic oxygen of the sugar moiety (22).

Clearly, however, a hydrogen bond to the ring oxygen of the proximal saccharide would be counter-catalytic since it would serve to destabilize the oxocarbenium ion-like transition state. It seems likely, therefore, that as the transition state is approached the hydrogen bond donated by the Tyr69 phenolic group becomes asymmetric, favoring Glu78 $\text{O}^{\epsilon 2}$. Simultaneously, the interaction between Tyr69 O^{η} and the partially positively charged O5 of the proximal xylose residue becomes a direct oxygen-oxygen contact, unmediated by a proton. A dipolar interaction could then form between the two oxygen atoms, concomitant with improved proton donation from Tyr69 to the partially negatively charged $\text{O}^{\epsilon 2}$ atom of Glu78, and, as such, could stabilize the transition state. This interaction may play an important role in catalysis and provide yet another explanation of the requirement of Tyr69 for enzyme activity.

A second interaction that differs substantially between the BCX-Xb and BCX-2FXb structures is that involving the $\text{O}^{\epsilon 1}$ of Glu78 and the 2-substituent of the proximal sugar (OH in the noncovalent complex and F in the covalent species). Despite the fact that the interaction between the fluorine and the oxygen in the covalent complex must be destabilizing, the distance between these two atoms is shorter than that seen for the analogous yet stabilizing hydrogen-bonding interaction in the BCX-Xb noncovalent complex (Table 3). The shortening of this distance in BCX-2FXb appears to be a consequence of the formation of the covalent bond at the anomeric center and the ${}^4C_1 \rightarrow {}^{2,5}B$ conformational change in the proximal saccharide. Similar interactions have been seen in other 2-fluorosugar glycosyl-enzyme complexes and may be an important component of catalysis with the natural substrate (20-22). The suggestion is that a short, strong hydrogen bond is formed at this position in the glycosyl-enzyme intermediate and that this hydrogen bond is even shorter and stronger at the transition state where it is optimized geometrically and electrostatically. This is consistent with the very strong transition-state interactions

(typically 20–40 kJ mol⁻¹) measured at the 2-position for a number of glycosidases and further bolstered by the recent observation of a very close ($d = 2.37 \text{ \AA}$) interaction between O^{ε1} of the nucleophile and the hydroxyl group at C2 of the substrate in the cellobiosyl-enzyme intermediate formed on a double mutant of *Cellulomonas fimi* Cex (39, 40). It is noteworthy that an essentially identical interaction is seen in the present case, even though BCX is from a different structural clan and the proximal saccharide is distorted.

Another residue interacting with the 2-position fluorine in the BCX–2FXb complex is the highly conserved Arg112 (Figure 5). This suggests an important role for this residue in hydrogen bonding to the 2-hydroxyl of natural substrates as has been proposed for Asn126 in *Cellulomonas fimi* Cex or Asn186 in *Sinapis alba* myrosinase (22, 40). It is, therefore, surprising that the mutation of this residue causes only relatively small deleterious effects on catalysis (R112K and R112N BCX have 83% and 35% of wild-type activity, respectively, toward xylan) (12). For BCX then, the most important interaction with the 2-substituent appears to be that with the O^{ε1} atom of Glu78.

The planar organization of the reaction center and the interactions with Tyr69 in BCX–2FXb appear to generate a much more reactive glycosyl-enzyme intermediate than those seen in the clan GH-A enzymes. This is consistent with kinetic observations since the deglycosylation step never became rate-limiting for wild-type BCX even when studied with highly reactive aryl xylobiosides (41). By contrast, the deglycosylation step for Cex is rate-limiting for all aryl cellobiosides and xylobiosides studied, implying a much slower deglycosylation step relative to glycosylation.

Interactions at C5 of the Proximal Saccharide and Substrate Specificity. Unlike the β-1,4-glycanases, such as *Cellulomonas fimi* Cex, which act on both xylan and cellulose, the family G/11 β-1,4 xylanases are specific for xylan (8, 41). Both the BCX–2FXb glycosyl-enzyme intermediate and the BCX–Xb noncovalent structures provide insight into this specificity. If the C5 atom of a xylose residue carried a hydroxymethyl group, as do the glucose residues of cellulose, there would be significant steric problems associated with accommodating the saccharide units into the active site cleft of BCX. Modeling experiments with both complex structures suggest that a hydroxymethyl group on the distal saccharide would clash with the carbonyl oxygen of Ser117, while, in the proximal saccharide, such a group would clash with the C^{γ2} atom of Val37. In fact, the C5 atom of the proximal saccharide in the glycosyl-enzyme intermediate makes three van der Waals interactions with the protein, contacting the C^{γ2} atom of Val37 ($d = 3.71 \text{ \AA}$), the C^{ε3} atom of Trp9 (3.59 Å), and the N^{δ2} atom of Asn35 ($d = 3.69 \text{ \AA}$). These contacts with C5 are more extensive than those seen between any other atom of this ligand and the protein and, together, appear to shape this portion of the active site cleft such that it limits substrates to those that are unsubstituted at the C5 position. Note also that achieving the ^{2,5}B conformation observed in the glycosyl-enzyme intermediate would be extremely difficult for glucose. This would force the bulky hydroxymethyl group into the flagstaff conformation with substantial steric costs, both between the sugar and the protein and within the sugar itself due to the “bowsprit” interactions with H2.

Implications. The observation of such striking conformational distortion for a sugar residue in a glycosyl-enzyme intermediate is unprecedented. Furthermore, the nature of this conformational distortion is matched in interest by its implications for the catalytic mechanism. The distortion to the ^{2,5}B conformation places C5, O5, C1, and C2 in a planar arrangement that would considerably facilitate the formation of oxocarbenium ion character at this center in the transition state. Interestingly, the same ^{2,5}B conformation was proposed previously as the conformation of the α-glucoside substrate bound to yeast α-glucosidase and identical arguments were forwarded concerning C5, O5, C1, and C2 (42). It was also pointed out that, in this conformation, there is no lone pair on the ring oxygen that is antiperiplanar to the scissile bond, whereas in the ⁴C₁ conformation such an arrangement does exist. The first step (glycosylation) for an α-glycosidase and the second step (deglycosylation) for a β-glycosidase have identical stereochemical outcomes (α → β), and thus stereoelectronic theory would apply in an equivalent manner to each. The direct observation of the saccharide bound to BCX in a ^{2,5}B conformation, therefore, provides substantial evidence against the importance of the antiperiplanar lone pair hypothesis of Deslongchamps as applied to glycosidases (43).

Complexes of glycosidases with substrate or with product in which a sugar ring is substantially distorted have been observed previously. The best defined are those in which the substrate is bound across the cleavage site with occupancy of both the -1 and +1 subsites, leading to the suggestion that interactions with the +1 subsite are driving the distortion (23, 44, 45). The degree of distortion in these complexes, however, as well as that seen in a hen egg white lysozyme product complex (46), is not as great as that seen in the present example. Further, it is important to note that, because such interactions do not exist in this case, +1 site interactions cannot be important in causing distortion for the covalent intermediate.

The van der Waals interactions of the C5 atom of the proximal xylose residue suggest not only that the active site is designed specifically for xylan hydrolysis but also that this atom may have a role in achieving the ^{2,5}B conformation. As this atom makes multiple contacts with the protein and occupies a similar position in both the BCX–Xb and the BCX–2FXb structures, it may provide a “hinge” for the action required to mediate distortion from the ⁴C₁ to the ^{2,5}B conformation (Figure 4c). Regardless, it is certain that the lack of the hydroxymethyl group at C5 is key to the ability to undergo this distortion, suggesting that the hydrolysis of glucose-based substrates by other β-1,4-glycosidases may follow a different course.

Some of the most important interactions at the active site of BCX appear to be those between the phenolic group of Tyr69 and the endocyclic (O5) oxygen of the proximal sugar ring and O^{ε2} of Glu78, as well as those between the 2-position of the proximal sugar and O^{ε1} of Glu78. Notably, the phenolic group of Tyr69, as determined from the structure of Y69F BCX, is not involved in correctly positioning the nucleophile or maintaining active site structural features. Instead, the interactions between Tyr69 and its hydrogen-bonding partners serves to form an extended network which appears to redistribute charge as it is developed at the transition state while at the same time stabilizing the required planar

structure. The structure of the BCX glycosyl-enzyme intermediate with its flattened oxocarbenium-like conformation provides insight into the mechanism of xylan hydrolysis and serves to highlight some of the important sites of interaction in a manner that may be useful for the engineering of xylanases for biotechnological applications.

ACKNOWLEDGMENT

We thank Lloyd Mackenzie for technical assistance and Greg Connelly and Manish Joshi for providing protein and insightful discussion.

REFERENCES

- Bernstein, F. C., Koetzle, T. F., Williams, G. J., Meyer, E. E., Jr., Brice, M. D., Rodgers, J. R., Kennard, O., Shimanouchi, T., and Tasumi, M. (1977) *J. Mol. Biol.* 112, 535–542.
- Henrissat, B., and Davies, G. (1997) *Curr. Opin. Struct. Biol.* 7, 637–644.
- Gebler, J., Gilkes, N. R., Claeysens, M., Wilson, D. B., Beguin, P., Wakarchuk, W. W., Kilburn, D. G., Miller, R. C., Jr., Warren, R. A., and Withers, S. G. (1992) *J. Biol. Chem.* 267, 12559–12561.
- Koshland, D. E. (1953) *Biol. Rev.* 28, 416–436.
- McCarter, J. D., and Withers, S. G. (1994) *Curr. Opin. Struct. Biol.* 4, 885–892.
- Paice, M. G., Gurnagul, N., Page, D. H., and Jurasek, L. (1992) *Enzyme Microb. Technol.* 14, 272–276.
- Coughlan, M. P., and Hazlewood, G. P. (1993) *Biotechnol. Appl. Biochem.* 17, 259–289.
- Törrönen, A., and Rouvinen, J. (1997) *J. Biotechnol.* 57, 137–149.
- Törrönen, A., and Rouvinen, J. (1995) *Biochemistry* 34, 847–856.
- Krengel, U., and Dijkstra, B. W. (1996) *J. Mol. Biol.* 263, 70–78.
- Campbell, R. L., Rose, D. R., Wakarchuk, W. W., To, R., Sung, W., and Yaguchi, M. (1993) in *Proceedings of the Second TRICEL Symposia on Trichoderma reesei and Other Hydrolases* (Suominen, P., and Reinikainen, T., Eds.) pp 63–72, Foundations for Biotechnical and Industrial Fermentation, Helsinki, Finland.
- Wakarchuk, W. W., Campbell, R. L., Sung, W. L., Davoodi, J., and Yaguchi, M. (1994) *Protein Sci.* 3, 467–475.
- Wakarchuk, W., Methot, N., Lanthier, P., Sung, W., Seligy, V., Yaguchi, M., To, R., Campbell, R., and Rose, D. (1992) in *Xylan and xylanases* (Visser, J., Ed.) pp 439–442, Elsevier Science, Amsterdam, The Netherlands.
- Withers, S. G., and Aebersold, R. (1995) *Protein Sci.* 4, 361–372.
- Miao, S., Ziser, L., Aebersold, R., and Withers, S. G. (1994) *Biochemistry* 33, 7027–7032.
- McIntosh, L. P., Hand, G., Johnson, P. E., Joshi, M. D., Korner, M., Plesniak, L. A., Ziser, L., Wakarchuk, W. W., and Withers, S. G. (1996) *Biochemistry* 35, 9958–9966.
- Havukainen, R., Törrönen, A., Laitinen, T., and Rouvinen, J. (1996) *Biochemistry* 35, 9617–9624.
- Withers, S. G., Street, I. P., Bird, P., and Dolphin, D. H. (1987) *J. Am. Chem. Soc.* 109, 7530–7531.
- Withers, S. G., Rupitz, K., and Street, I. P. (1988) *J. Biol. Chem.* 263, 7929–7932.
- White, A., Tull, D., Johns, K., Withers, S. G., and Rose, D. R. (1996) *Nat. Struct. Biol.* 3, 149–154.
- Notenboom, V., Birsan, C., Warren, R. A. J., Withers, S. G., and Rose, D. R. (1998) *Biochemistry* 37, 4751–4758.
- Burmeister, W. P., Cottaz, S., Driguez, H., Iori, R., Palmieri, S., and Henrissat, B. (1997) *Structure* 5, 663–675.
- Davies, G. J., Mackenzie, L. F., Varrot, A., Dauter, M., Brzozowski, A. M., Schülein, M., and Withers, S. G. (1998) *Biochemistry* 37, 11707–11713.
- Ziser, L., Setyawati, I., and Withers, S. G. (1995) *Carbohydr. Res.* 274, 137–153.
- Otwinowski, Z., and Minor, W. (1997) *Methods Enzymol.* 276, 307–326.
- Brünger, A. T. (1992) *X-PLOR Version 3.1: A system for X-ray crystallography and NMR*, Yale University Press, New Haven, CT.
- Collaborative Computational Project Number 4 (1994) *Acta Crystallogr., Sect. D* 50, 760–763.
- Jones, T. A., Zhou, J.-Y., Cowan, S. W., and Kjeldgaard, M. (1991) *Acta Crystallogr., Sect. A* 47, 110–119.
- Luzzati, P. V. (1952) *Acta Crystallogr., Sect. A* 50, 803–810.
- Davies, G. J., Wilson, K. S., and Henrissat, B. (1997) *Biochem. J.* 321, 557–559.
- IUPAC–IUB (1980) *Eur. J. Biochem.* 111, 295–298.
- Vyas, N. K. (1991) *Curr. Opin. Struct. Biol.* 1, 732–740.
- Sinnott, M. L. (1990) *Chem. Rev.* 90, 1171–1202.
- Stoddart, J. F. (1971) *Stereochemistry of Carbohydrates*, John Wiley and Sons, New York.
- Joshi, M. D., Hedberg, A., and McIntosh, L. P. (1997) *Protein Sci.* 6, 2667–2670.
- Gebler, J. C., Trimbur, D. E., Warren, A. J., Aebersold, R., Namchuk, M., and Withers, S. G. (1995) *Biochemistry* 34, 14547–14553.
- Baker, E. N., and Hubbard, R. E. (1984) *Prog. Biophys. Mol. Biol.* 44, 97–179.
- Jones, P. G., and Kirby, A. J. (1984) *J. Am. Chem. Soc.* 106, 6207–6212.
- Namchuk, M. N., and Withers, S. G. (1995) *Biochemistry* 34, 16194–16202.
- Notenboom, V., Birsan, C., Nitz, M., Rose, D. R., Warren, R. A. J., and Withers, S. G. (1998) *Nat. Struct. Biol.* 5, 812–818.
- Tull, D., and Withers, S. G. (1994) *Biochemistry* 33, 6363–6370.
- Hosie, L., and Sinnott, M. L. (1985) *Biochem. J.* 226, 437–446.
- Deslongchamps, P. (1983) *Stereoelectronic effects in organic chemistry*, 1st ed., Pergamon Press, Oxford; New York.
- Sulzenbacher, G., Driguez, H., Henrissat, B., Schülein, M., and Davies, G. J. (1996) *Biochemistry* 35, 15280–15287.
- Tews, I., Perrakis, A., Oppenheim, A., Dauter, Z., Wilson, K. S., and Vorgias, C. E. (1996) *Nat. Struct. Biol.* 3, 638–648.
- Strynadka, N. C., and James, M. N. (1991) *J. Mol. Biol.* 220, 401–424.
- Kraulis, P. J. (1991) *J. Appl. Crystallogr.* 24, 946–950.
- Merritt, E. A., and Murphy, M. E. P. (1994) *Acta Crystallogr., Sect. D* 50, 869–873.
- McDonald, I. K., and Thornton, J. M. (1994) *J. Mol. Biol.* 238, 777–793.
- Wallace, A. C., Laskowski, R. A., and Thornton, J. M. (1995) *Protein Eng.* 8, 127–134.

BI982946F